Mongolian Journal of Chemistry
www.mongoliajol.info/index.php/MJC

Preparation of catalyst from natural montmorillonite mineral and its application in the synthesis of carbon nanosphere

Altantuya Ochirkhuyag[1*], Ulambayar Rentsennorov[1], Davaabal Batmunkh[1], Oyun-Erdene Gendenjamts[1], Enkhtur Odbaatar[3], Tserendagva Tsend-Ayush[3], Jadambaa Temuujin[1,2]

[1]Institute of Chemistry and Chemical Technology,
Mongolian Academy of Sciences, Ulaanbaatar, 13330, Mongolia
[2]CITI University, Ulaanbaatar, 14190, Mongolia
[3]Erdenet Mining Institute, Erdenet, 61027, Mongolia

** Corresponding author: altantuya_o@mas.ac.mn;* ORCID ID: 0000-0001-6495-7360

Received: 28 November 2022; revised: 15 December ; accepted: 20 December 2022

ABSTRACT

In developed countries, nanoparticles derived from natural minerals and high-purity chemicals both are widely studied, while in developing countries like Mongolia, the natural minerals-based nanoparticles have more interest because of the low production cost and applicability of domestic natural minerals for their production. For the synthesis of natural mineral-based nanomaterials, it is important first to define the chemical composition and physical structure of local minerals and their possible processing route. We employed an environmentally friendly alkaline leaching procedure to recover silica from the clay mineral at 90°C for 24 hours. We applied an organic surfactant (CTAB) and a simple coprecipitation approach to form iron-doped silica nanoparticles. Consequently, we used iron-doped silica nanoparticles as a substrate and catalyst for the synthesis of carbon nanosphere at 750 °C for 1 hour in an argon and acetylene gas atmosphere. As a result, vast quantities of superhydrophobic carbon nanospheres (CNS) were obtained. The physicochemical properties of nanosilica substrate, non-functionalized carbon nanosphere, and functionalized carbon nanosphere (CNS) samples were characterized using XRD, XRF, SEM, EDS, TEM, and FTIR spectrometer. Iron-doped mineral-derived nanosilica particles demonstrated high catalytic efficiency and the potential to produce a large amount of value-added carbon nanospheres. Superhydrophobic CNS can be used in a variety of applications, particularly drug delivery; however, to use CNS in both aqueous and non-aqueous media, the superhydrophobic properties of CNS can be modified using different oxidizers. The changes in hydrophobicity of the CNS were examined and suggested possible oxidizing agents.

Keywords: Silica, carbon nanosphere, mineral, nanoparticle, catalyst

INTRODUCTION

Clay minerals belong to the most abundant sedimentary mineral group. They are classified as phyllosilicates and predominate in colloidal fractions of soils, sediments, rocks, and waters (usually hydrous aluminosilicates). There are several types of geological environments for the natural growth of clay minerals: weathering, sedimentation, burial-diagenetic and hydrothermal. The conditions for clay mineral formation differ in different environments, resulting in differences in the chemical composition, crystal morphology, mechanical, and textural properties of respective deposits [1]. Clay mineral deposits are evenly distributed throughout Mongolia, with over 50 deposits discovered. Layers of $Si(O,OH)_4$ tetrahedra and layers of $M(OH)_6$ octahedra make up clay mineral platelets, where M is a divalent or trivalent cation. Only the mode of crystal sheet stacking, nature of bonding, and type of cation in the lattice induces different clay minerals, such as kaolinite, montmorillonite, and illite. Montmorillonite is a smectite group mineral composed of two silica-based tetrahedral sheets with water molecules within the interlayer sheets (2:1 structure) [2] that are easily accessible to inbound compounds. This ion exchange property makes montmorillonite minerals suitable for a variety of applications.

Instead of using expensive chemical grade precursors, the use of naturally abundant minerals as precursors for the synthesis of value-added materials such as catalysts is the crucial factor for their application.

Catalysts are used in more than 80 % of all industrial processes, including the generation of electrical energy, the removal of pollutants from the environment, and the synthesis of advanced materials for rapidly expanding electronic applications [3]. Superconductive carbon nanomaterials including carbon nanotubes, graphene, graphene oxide, fullerene, and carbon nanospheres have become one of the most sought-after materials at present due to their electrochemical properties, electronic abilities, large surface area, and resistance to extreme temperatures and pressures [4]. They are used in a wide range of applications including aerospace and defence, automotive, energy, construction, electronics, and imaging [5].

Among them, carbon nanospheres (CNS) have a large surface area, uniform size and shape, and a small energy band gap, which enables them to be used in a variety of applications such as heavy metal removal, organic pollutant removal, drug delivery, electronic conductor, filler material for various construction materials, sensors, photo-catalysis, and optoelectronic devices [6, 7]. Super hydrophobic carbon nanospheres have emerged as a promising candidate for extremely diluted solutions, separate biological mixtures, improve ultrasensitive molecular spectroscopy, actively convey, and organize molecules at the nanoscale level, provide smart chambers for chemical reactions, and controlled drug release [8, 9] and drug delivery in cancer cell treatment [10]. It is possible to change a surface by attaching a carboxyl or hydroxyl group and increasing the hydrophilic property of the material, allowing CNS to be used in an even broader range of applications. In addition, most studies on carbon nanosphere synthesis used chemical-grade precursors as a catalyst for the chemical vapour deposition (CVD) method [11]. There have only been a few attempts to use natural minerals such as laterite and kaolin as a substrate or catalyst in the synthesis of carbon nanospheres but montmorillonite [12, 13].

In this study, we synthesized carbon nanospheres for the first time using a domestic mineral as a support/ catalyst. Various characterization techniques, such as XRD, SEM-EDS, TEM, and FTIR, were used to reveal the physicochemical properties of the synthesized CNS. In addition, the surface properties of CNS, such as hydrophobicity, were studied, and acid activation was used to increase hydrophilic properties, increasing the possibility of using this final product in more diverse applications in aqueous and non-aqueous environments.

EXPERIMENTAL

Mineral source and properties of the montmorillonite mineral: More than 50 various clay mineral deposits have been discovered in Mongolia, and our sample was taken from the Humeltei montmorillonite deposit, which is located 50 kilometres east of Ulaanbaatar in the Tuv aimag. The mineral was grey-white and was collected as a fine powder. The general composition of Humeltei montmorillonite mineral is 55 wt.% SiO_2, 17 wt.% Al_2O_3, 7 wt.% K_2O, 2 wt.% FeO, and about 5 wt.% organic component (Figure S1). Analytical grade sodium hydroxide (NaOH) and iron III chloride ($FeCl_3 \times 6H_2O$) were purchased from Xilong Scientific Co.,Ltd, and hexadecyl trimethyl ammonium bromide (CTAB) was purchased from *Rhawn Chemical* Technology Co., Ltd.

Synthesis of catalyst: Montmorillonite mineral was mechanically milled in 30 minutes on a vibration mill (VM-4, Czechoslovakia) and sieved with 0.075 mm mesh. To extract silicon, 10 g of the mechanically milled mineral was added to 100 ml of 3 M sodium hydroxide solution for 24 hours at 90 °C. The 50 ml of the extracted alkaline solution is then mixed with 2 g of CTAB to increase surface area and porosity of silica nanoparticle [14, 15] and 0.5 g $FeCl_3$ dissolved in 40 ml distilled water for 4 hours while being constantly stirred. Then 2M of H_2SO_4 was added dropwise to the mixture until silica precipitation occurs at pH 6 and mixed again 30 minutes to stabilize the system. After that, the mixture was placed in a Teflon vessel for 24 hours at 100 °C to support CTAB-SiO_2 compound forms. Following that, the mixture is filtered through a 0.45-micron nylon filter and repeatedly washed with ethanol and water. The filtrate was dried at 110 °C for 2 hours to remove the water content and then heated at 550 °C for hours to remove the surfactant CTAB and create a porous silica surface.

Synthesis of CNS: On the ceramic boat, 0.3 g of catalyst is placed and inserted into the furnace (400-1 Nabertherm, Germany). Before the oven temperature reached 750 °C, argon gas was added to the system to remove oxygen. In 1 hour at 750 °C, acetylene gas and argon gas at a flow rate of 1:10 passed through the furnace tube. Following the reaction, the acetylene gas was turned off and only argon gas was allowed to flow until the furnace temperature reached room temperature (Figure 1a).

Surface functionalization of CNS: A. HNO_3: In 24 hours of constant stirring, 0.1 g of CNS sample was oxidized by 50 ml of 5M HNO3. The dispersion was filtered, and the oxidized CNS was washed with distilled water until pH 7 before drying for 2 hours at 110 °C.

B. $KMnO_4$: 0.1 g of CNS was oxidized by sonication with 0.225 g of $KMnO_4$ (potassium permanganate) and 0.2 M H_2SO_4 in 4 hours. The mixture was filtered and treated CNS was washed with distilled water until pH neutral and dried at 110 °C for 2 hours.

Suspension with Pluronic F68: A single rapid test for 50 ml of 0.5% Pluronic F68 solution and 0.007 g of CNS with sonication for 1 hour was performed. The suspension was then placed in a room, and the settlement of CNS particles was photographed at various times (1 hour, 24 hours, and 48 hours).

Experimental techniques: The chemical composition of the original mineral was detected by handheld X-ray

Fluorescence spectrometry (SkyRay Instrument). For crystal structure characterization, a Rigaku Miniflex II powder X-ray diffractometer with a Cu K radiation source (I = 0.15418 nm) operating at 30 kV and 15 mA at room temperature and a scanning rate of 0.5-degree min1 in the 10-70° 2θ range was used. CNS surface modification was investigated using Fourier-Transform Infrared (FTIR) spectroscopy (IR Prestige-21). To perform compositional studies, a high-resolution Transmission Electron Microscope HR-TEM (FEI TECNAI G2 20 X-TWIN) with an accelerating voltage of 200 kV and a Scanning Electron Microscope (Hitachi S-4700Type II instrument (30 kV accelerating voltage) integrated with EDS were used. SEM (TESCAN TIMA3) was also used to perform morphological studies on some samples. The Image J program was used to examine the size distribution of the CNS on a TEM image.

RESULTS AND DISCUSSIONS

X-ray diffractometry analysis results are shown in Fig. 1b. Reflection peaks were appeared at 20°, 26.6°, 27.9°, 32° and 34.9° 2θ for montmorillonite sample. Mineral montmorillonite-associated peaks have appeared at 20°, 28° and 36° 2θ and quartz peak appeared at 26.6° 2θ [16]. Unlikely Fe-SiO_2 sample was showed strong and broad peak at 15-18° 2θ which corresponds to nano SiO_2 (101) [17]. Other peaks have appeared at 34° and 36° 2θ which explains the possibility of the formation of iron oxide (Fe_3O_4) after heat treatment at 550 °C for removal of surfactant CTAB in catalyst structure [18]. As synthesized CNS sample showed carbon sphere-associated reflection peaks at 24.8°, 41.7°, and 42.7° 2θ [19] and peaks at 48.5° and 62.1° 2θ which are related to metallic iron formation due to high-temperature synthesis condition in reducing atmosphere [20].

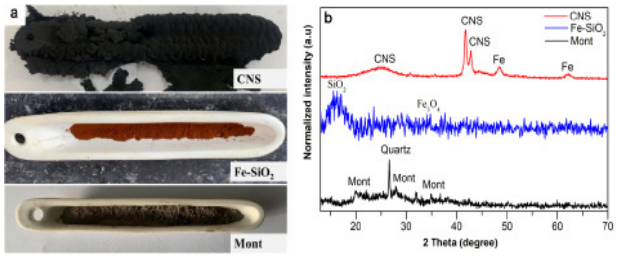

Fig. 1. Montmorillonite mineral, catalyst prior to furnace placement and CNS formation on the catalyst (a), and X-ray diffractograms of montmorillonite mineral, Fe-SiO2 catalyst and CNS (b).

The chemical composition of the samples is shown in Fig. S2. According to elemental analysis, the mechanically processed montmorillonite mineral sample was containing oxygen 44 wt.%, silicon 17.6 wt.%, aluminium 9.3 wt.%, organic carbon 9.2 wt.%, iron 5.7 wt.%, zinc 3.3 wt.%, potassium 2.2 wt.%, sodium 1.1 wt.%, and minor elements less than 1 wt.% including magnesium, phosphorus, titanium, calcium, chlorine etc. Fe-SiO_2 sample was containing oxygen 44 wt.%, silica 12.8 wt.%, aluminium 7.2 wt.%, iron 19.4 wt.%, sodium 1.6 wt.% and most of the impurities like magnesium, chlorine, potassium, calcium, titanium, zinc was not present in the catalyst/support sample. As-synthesized CNS sample was mostly containing carbon 77.6 wt.%, oxygen 20.7 wt.%. However, iron 0.1 wt.%, aluminium 0.1 wt.%, and silicon 0.07 wt.% impurities were present in the sample derived from the catalyst/support [21], and except for these negligible amounts of elements from the catalyst/support, CNS demonstrated high purity.

Morphological information of the samples was revealed by SEM and an image of the samples is shown in Fig. 2. Mechanically milled and sieved by 0.075 mm sample showing 1–10-micron sized particles which are aggregated together (Fig. 2a). It is clear that due to mechanical processing particle size of the mineral was decreased significantly purpose to increase the dissolution rate in alkaline media. Fig. 2b shows the morphology of the sample Fe-SiO_2, and the distribution of particles was even, and the size of the particle looks smaller than 1 micron. In Fig. 2c, the morphology of the CNS sample and it is visible that sphere-shaped carbon particles were formed. It was also interesting to note that those sphere-shaped particles were connected and created chains of beads-like accretions of the carbon spheres [22].

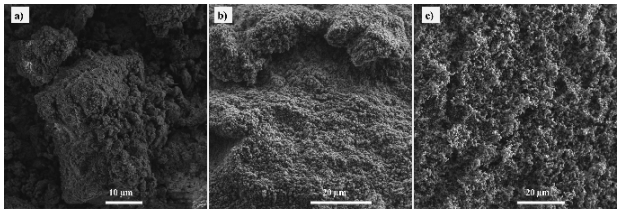

Fig. 2. SEM image of montmorillonite mineral (a), Fe-SiO_2 catalyst/support (b), and CNS (c).

Particle shape and size distribution of the samples revealed by TEM. Fig. S3 shows the porous silica particles as substrate and darker particles on the silica structure were iron oxide particles with the size of 20 nm to 100 nm. Further, the particle shape and size of the final product CNS is revealed in Fig. 3. According to the TEM image (Fig. 2a), CNS is contained with a spherical shape and particle size ranges from 5 nm to 100 nm [23]. The particle size distribution was analyzed by the Image J program, and the histogram shows that 125 particles were analyzed, with an average particle size of 9.96 nm (Fig. 3b). TEM images show particles as small as 10-20 nm, whereas SEM images show larger spheres (Fig. 2c). As a result, we expect larger aggregated CNS particles to be separated during sample preparation for TEM measurement using sonication in acetone.

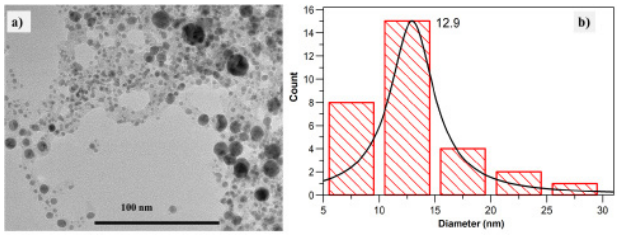

Fig. 3. TEM image of the CNS sample (a) and size distribution histogram detected by Image J program (b).

Surface properties and functionalization of Carbon Nanosphere; The functional groups of the pre-pared nanospheres were detected by Fourier transform infrared (FTIR). Figure 4 shows the FTIR spectrum of CNS and acid functionalized 2 samples. The spectrum of CNS pristine shows a broad and strong peak at 3438 cm^{-1} which is shifted in the other two acid-treated samples to 3445 cm^{-1}. This shifted peak at 3445 cm^{-1} ascribed to -OH band [24]. It has another 6 major peaks at 674 cm^{-1}, 812 cm^{-1}, 1629 cm^{-1}, 1709 cm^{-1}, 2364 cm^{-1}, 2858 cm^{-1}, 2924 cm^{-1} same as other two samples. O-H stretching vibrations overlap with C-H stretching vibrations, typically for alkyl groups at wavenumbers 2975 to 2845 cm^{-1}. In functionalized CNS, the peak at 1364 cm-1 is due to C–OH stretching vibrations and the peak at 1028 cm^{-1} and 978 cm^{-1} is due to C–O stretching vibrations. O-H vibration band at wavenumber ~900 cm^{-1}. The additional absorption band at wavenumber ~1741 cm^{-1} is due to the stretching vibration of the C=O (carbonyl group) for both functionalized samples [25].

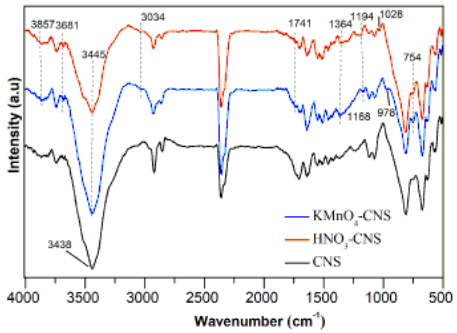

Fig. 4. FTIR spectra of pristine CNS, HNO_3 activated CNS and $KMnO_4$ activated CNS.

The ability of the CNS sample to suspend in aqueous media also confirmed its functionalization, as shown in Fig. 5. Super-hydrophobic CNS did not disperse well in water and only a small amount of particle was suspended after 1 hour of sonication (sample №1 in Fig. 5a), whereas HNO_3 and $KMnO_4$ activated CNS samples demonstrated high dispersion ability at the same time (samples №2 and №3, respectively in Fig. 5a). After 24 hours, the pristine CNS sample had completely settled on the bottom. The HNO_3 and $KMnO_4$ treated CNS samples were still visibly dispersed in the system, but some particles had settled in the bottom as well (Fig. 5b). Interestingly, the HNO_3-treated CNS sample was still dispersed in the system after 48 hours, implying that more changes in the hydrophobicity of the CNS surface occurred than that (Fig. 5c). The results show that it is possible to increase the hydrophilic property of CNS by using a longer oxidizer treatment time. However, when compared to the literature of similar carbon nano materials [26, 27], both treatments took less time and produced promising results. Another quick and simple test with Pluronic F68 and CNS sample revealed that CNS dispersion in water was significantly increased and remained stable for 48 hours, similar to the HNO_3-treated CNS sample (Fig. S4). The results indicate that CNS with Pluronic surfactant could be used in fields other than adsorption, particularly biology and biomedicine [28, 29].

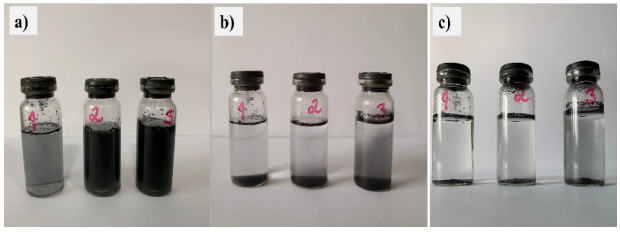

Fig. 5. Pristine CNS- sample №1, $KMnO_4$ - H_2SO_4 activated CNS- sample №2, HNO_3 activated CNS - sample №3 after 1 hour sonication (a), 24 hours (b), and 48 hours later (c).

Furthermore, CNSs are negatively charged, and they can be changed while modifying with surfactants (anionic and cationic) [30]. As a result, CNSs modified with surfactant exhibit good stability. According to these findings, we can use as-synthesized CNS for cationic dye adsorption (Methylene Blue, Rhodamine B) [31] and transportation fuel desulfurization [32] or modify it with a surfactant and then use modified CNS for anionic dye adsorption (Methyl Orange, Alizarin Yellow).

CONCLUSIONS

The use of the natural mineral montmorillonite as a precursor to creating substrate and catalyst for CNS synthesis was completed successfully. As the demand for superhydrophobic nanomaterials grows, CNS can be used directly in those applications. In the case of aqueous media application, acid treatments demonstrated the ability to change the super hydrophobic property of the CNS. This study also demonstrated the potential of montmorillonite mineral-derived nanomaterials in a variety of applications.

ACKNOWLEDGEMENTS

The authors gratefully acknowledge the support for this work from the “Study and application of nano functional material synthesis from natural mineral raw material”, 2019-2022 research grant funded by the Mongolian Foundation for Science and Technology, Ministry of

Education, Culture, Science and Sports of Mongolia. The authors would also like to thank the Department of Applied and Environmental Chemistry at the University of Szeged for their support in characterizing the samples using SEM, TEM, and XRD.

REFERENCES

1. Čejka J., Roth W.J., Opanasenko M. (2017). Two-dimensional silica-based inorganic networks. In: Jerry L. Atwood (ed.) Comprehensive supramolecular chemistry II, Elsevier, 475-501. https://doi.org/10.1016/B978-0-12-409547-2.13647-9
2. Haldar S.K., Tišljar J. (2014). Basic Mineralogy. In: Introduction to mineralogy and petrology. Chapter II, Elsevier, 39-79. https://doi.org/10.1016/B978-0-12-408133-8.00002-X
3. Moulijn J.A., van Leeuwen P.W.N.M., van Santen R.A. (1993). Catalytic processes in industry. In: Studies in surface science and catalysis. Chapter II, Elsevier, 23-67. https://doi.org/10.1016/S0167-2991(08)63806-9
4. Ashutosh Tiwari, Shukla S.K. (2014). Advanced carbon materials and technology. John Wiley & Sons, Inc. 1-514. https://doi.org/10.1002/9781118895399
5. Fang Y., Guo S., Li D., Zhu C., Ren W., *et al*. (2012). Easy synthesis and imaging applications of cross-linked green fluorescent hollow carbon nanoparticles. *ACS Nano*, **6**(1), 400-409. https://doi.org/10.1021/nn2046373
6. Zhao H., Zhang F., Zhang S., He S., Shen F., *et al*. (2018). Scalable synthesis of sub-100 nm hollow carbon nanospheres for energy storage applications. *Nano Res.*, **11**, 1822-1833. https://doi.org/10.1007/s12274-017-1800-3
7. Nieto-Márquez A., Romero R., Romero A., Valverde, J.L. (2011). Carbon nanospheres: Synthesis, physicochemical properties and applications. *J. Mater. Chem.*, **21**(6), 1664-1672. https://doi.org/10.1039/C0JM01350A
8. Ciasca G., Papi M., Businaro L., Campi G., Ortolani M., *et al.* (2016). Recent advances in superhydrophobic surfaces and their relevance to biology and medicine. *Bioinspir. Biomim.,* **11**(1). https://doi.org/10.1088/1748-3190/11/1/011001
9. Aljumaily M.M., Alsaadi M.A., Das R., Abd Hamid S.B., Hashim N.A., *et al.* (2018). Optimization of the synthesis of superhydrophobic carbon nanomaterials by chemical vapor deposition. *Sci. Rep.*, **8**(1). https://doi.org/10.1038/s41598-018-21051-3
10. Kim T.W., Chung P.W., Slowing I.I., Tsunoda M., Yeung E.S., *et al.* (2008). Structurally ordered mesoporous carbon nanoparticles as transmembrane delivery vehicle in human cancer cells. *Nano Lett.*, **8**(11), 3724-3727. https://doi.org/10.1021/nl801976m
11. Ghaemi F., Yunus R., Jassim L., Ahmadian A., Ismail F. (2015). Synthesis of carbon nanotube-carbon nanosphere on the CF surface by CVD. *Advanced Mater. Res.,* **1134**, 209-212. https://doi.org/10.4028/www.scientific.net/AMR.1134.209
12. Kumar A., Kostikov Y., Orberger B., Nessim G.D., Mariotto G. (2018). Natural laterite as a catalyst source for the growth of carbon nanotubes and nanospheres. *ACS Appl. Nano Mate.*, **1**(11), 6046-6054. https://doi.org/10.1021/acsanm.8b01117
13. Miao J.Y., Hwang D.W., Narasimhulu K.V., Lin P.I., Chen Y.T., *et al.* (2004). Synthesis and properties of carbon nanospheres grown by CVD using Kaolin supported transition metal catalysts. *Carbon*, **42**(4), 813-822. https://doi.org/10.1016/j.carbon.2004.01.053
14. Poyraz A. ., Dag Ö. (2009). Role of organic and inorganic additives on the assembly of CTAB-P123 and the morphology of mesoporous silica particles. *Journal of Physical Chemistry C*, *113*(43), 18596-18607. https://doi.org/10.1021/jp907303a
15. Kim M.K., Ki D.H., Na Y.G., Lee H.S., Baek J.S., *et al.* (2021). Optimization of mesoporous silica nanoparticles through statistical design of experiment and the application for the anticancer drug. *Pharmaceutics*, **13**(2). https://doi.org/10.3390/pharmaceutics13020184
16. Djowe A.T., Laminsi S., Njopwouo D., Acayanka E., Gaigneaux E.M. (2013). Surface modification of smectite clay induced by non-thermal gliding arc plasma at atmospheric pressure. *Plasma Chem. Plasma Process.*, **33**(4), 707-723. https://doi.org/10.1007/s11090-013-9454-8
17. Maddalena R., Hall C., Hamilton A. (2019). Effect of silica particle size on the formation of calcium silicate hydrate [C-S-H] using thermal analysis. *Thermochimica Acta*, *672*, 142-149. https://doi.org/10.1016/j.tca.2018.09.003
18. Marsh A., Heath A., Patureau P., Evernden M., Walker P. (2018). Alkali activation behaviour of un-calcined montmorillonite and illite clay minerals. *Applied Clay Science*, *166*, 250-261. https://doi.org/10.1016/j.clay.2018.09.011
19. Zhuang L., Zhang W., Zhao Y., Shen H., Lin H., Liang J. (2015). Preparation and characterization of Fe_3O_4 particles with novel nanosheets morphology and magnetochromatic property by a modified solvothermal method. *Sci. Rep.*, **5**. https://doi.org/10.1038/srep09320
20. Pol V.G., Pol S.V., Calderon Moreno J.M., Gedanken A. (2006). High yield one-step synthesis of carbon spheres produced by dissociating individual hydrocarbons at their autogenic pressure at low temperatures. *Carbon*, **44**(15), 3285-3292. https://doi.org/10.1016/j.carbon.2006.06.023
21. Zhao N., Wang J., Shi C., Liu E., Li J., He C. (2014). Chemical vapor deposition synthesis of carbon

nanospheres over Fe-based glassy alloy particles. *Journal of Alloys and Compounds*, *617*, 816-822. https://doi.org/10.1016/j.jallcom.2014.08.072

22. Hussain N., Alwan S., Alshamsi H., Sahib I. (2020). Green synthesis of S- and N-codoped carbon nanospheres and application as adsorbent of Pb (II) from aqueous solution. *International Journal of Chemical Engineering*, **2020**. https://doi.org/10.1155/2020/9068358
23. Boufades D., Hammadou S., Mesdour N., Moussiden A., Benmebrouka H., *et al*. One-step synthesis and characterization of carbon nanospheres via natural gas condensate pyrolysis. *Fullerenes, Nanotubes and Carbon Nanostructures*, **28**(9), 716-723. https://doi.org/10.1080/1536383X.2020.1750383
24. Azri F.A., Sukor R., Hajian R., Yusof N. A., Bakar F.A., *et al.* (2017). Modification strategy of screen-printed carbon electrode with functionalized multi-walled carbon nanotube and chitosan matrix for biosensor development. *Asian Journal of Chemistry*, **29**(1), 3136. https://doi.org/10.14233/ajchem.2017.20104
25. Trykowski G., Biniak S., Stobinski L., Lesiak B. (2010). Preliminary investigations into the purification and functionalization of multiwall carbon nanotubes. 118. In *Acta Physica Polonica A*, **118**(3), 515-518. https://doi.org/10.12693/APhysPolA.118.515
26. Slobodian P., Riha P., Olejnik R., Cvelbar U., Saha P. (2013). Enhancing effect of $KMnO_4$ oxidation of carbon nanotubes network embedded in elastic polyurethane on overall electro-mechanical properties of composite. *Composites Science and Technology*, 81, 54-60.
27. Santangelo S., Messina G., Faggio G., Abdul Rahim S.H., Milone C. (2012). Effect of sulphuric-nitric acid mixture composition on surface chemistry and structural evolution of liquid-phase oxidised carbon nanotubes. *Journal of Raman Spectroscopy*, **43**(10), 1432-1442. https://doi.org/10.1002/jrs.4097
28. Ciofani G., Raffa V., Pensabene V., Menciassi A., Dario P. (2009). Dispersion of multi-walled carbon nanotubes in aqueous pluronic F127 solutions for biological applications. *Fullerenes Nanotubes and Carbon Nanostructures*, **17**(1), 11-25. https://doi.org/10.1080/15363830802515840
29. Gu J., Su S., Li Y., He Q., Shi J. (2011). Hydrophilic mesoporous carbon nanoparticles as carriers for sustained release of hydrophobic anti-cancer drugs. *Chemical Communications*, **47**(7), 2101-2103. https://doi.org/10.1039/C0CC04598E
30. Singhal S., Dixit S., Shukla A.K. (2019). Structural analysis of carbon nanospheres synthesized by CVD: an investigation of surface charges and its effect on the stability of carbon nanostructures. *Applied Physics A: Materials Science and Processing*, **125**(80). https://doi.org/10.1007/s00339-018-2372-0
31. Hoc Thang N., Sy Khang D., Duy Hai T., Thi Nga D., Dinh Tuan P. (2021). Methylene blue adsorption mechanism of activated carbon synthesised from cashew nut shells. *RSC Advances*, **11**(43), 26563-26570. https://doi.org/10.1039/D1RA04672A
32. Hammadou née Mesdour S., Boufades D., Bousak H., Moussiden A., Benmabrouka H., *et.al*. (2022). Potential application of carbon nanospheres as adsorbent for the simultaneous desulfurization and demetallization of transportations fuels. *Fullerenes Nanotubes and Carbon Nanostructures*, **30**(4), 419-427. https://doi.org/10.1080/1536383X.2021.1947809